CHAPTER SIX

Literal (Symbolic) Solutions for Three-Conductor Lines

The previous chapters have considered the solution of the MTL equations for a general $(n + 1)$-conductor line. In general, this solution process must be accomplished with digital computer programs; i.e., a numerical result is obtained. Although exact, this numerical process does not reveal the general behavior of the solution. In other words, the only information we obtain is the solution for the specific set of input data, e.g., line length, terminal impedance levels, source voltages, frequency, etc. In order to understand the general behavior of the solution, it would be helpful to have a *literal solution* for the induced crosstalk voltages in terms of the *symbols* for the line length, terminal impedances, per-unit-length capacitances and inductances, the source voltage, etc. From such a result we could observe how changes in some or all of these parameters would affect the solution. This advantage is similar to a transfer function which is useful in the design and analysis of electric circuits and automatic control systems [A.2]. In order to obtain this same insight from the numerical solution we would need to perform a large set of computations with these parameters being varied over their range of anticipated values.

Such transmission-line literal transfer functions for the prediction of crosstalk have been derived in the past for use in the frequency-domain analysis of microwave circuits [1–4] or for time-domain analysis of crosstalk in digital circuits [5–11]. However, all of these methods make one or more of the following assumptions about the line in order to simplify the derivation:

1. The line is a *three-conductor line*, i.e., $n = 2$, with two signal conductors and a reference conductor.
2. The line is *symmetric*, i.e., the two signal conductors are identical in cross-sectional shape and are separated from the reference conductor by identical distances.

3. The line is *weakly coupled*, i.e., the effect of the induced signals in the receiving circuit on the driven circuit is neglected (widely separated lines tend to satisfy this in an approximate fashion the wider the separation).
4. Both lines are *matched* at both ends, i.e., the line is terminated at all four ports in the line characteristic impedances.
5. The line is *lossless*, i.e., the conductors are perfect conductors and the surrounding medium is lossless.
6. The medium is *homogeneous*.

The obvious reason why these assumptions are used is to simplify the difficult manipulation of the *symbols* that are involved in the literal solution. The assumption of a symmetric line and the subsequent literal solution is referred to in the microwaves literature as the *even-odd mode solution*. However, numerous applications are not symmetric nor perfectly matched.

The purpose of this chapter is to derive the *literal* or *symbolic solution of the MTL equations for a three-conductor line* and to *incorporate the terminal impedance constraints into this solution* to yield *explicit equations for the crosstalk*. Both the frequency-domain and the time-domain solutions will be obtained. In addition, the derivation will not presume a symmetric line nor will it presume a matched line. We presume that the entries in the per-unit-length parameter matrices, **L** and **C**, are known. The idea is to simply proceed through the usual solution steps that would be involved in a numerical solution but instead to use symbols for all quantities rather than numbers. It is important to remind the reader of the steps to be taken. First we solve for the general solution in terms of $2n$ (4 in this case) undetermined constants and then we incorporate the terminal constraints in order to evaluate these undetermined constants. For a three-conductor line the last step, incorporation of the terminal conditions, involves the simultaneous solution of symbolic equations with, for example, Cramer's rule, and is quite difficult. It therefore does not appear to be feasible to extend this to lines consisting of more than three conductors. Even for a three-conductor line, the solution effort is so great that we must make some other simplifying assumptions. The primary simplification is to assume a *homogeneous surrounding medium* so that we may take advantage of the important identity for a homogeneous medium, $\mathbf{LC} = \mu\varepsilon\mathbf{1}_2$. This identity essentially reduces the number of symbols and allows the consolidation of certain other groups of the per-unit-length symbols. To further aid in simplification we first assume a lossless line; perfect conductors in a lossless, homogeneous medium. We then extend this result in an approximate fashion to consider imperfect conductors.

Besides providing considerable insight into the effect of each parameter on the solution, this literal solution also provides verification of some long-held intuitive notions. The first is that for an electrically short, weakly coupled line *and* a sufficiently small frequency, the total crosstalk can be written as the sum of two contributions. One contribution is due to the mutual inductance between

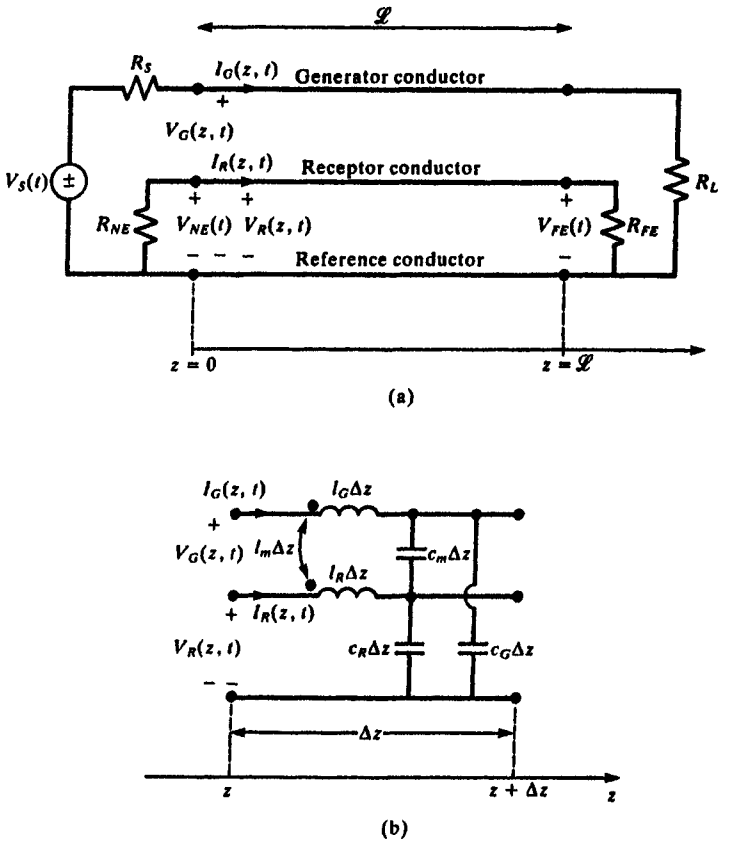

FIGURE 6.1 The three-conductor MTL: (a) line dimensions and terminal characterization and (b) the per-unit-length equivalent circuit.

the two circuits and the other is due to the mutual capacitance between the two circuits. This is the basis for the widely used, *inductive-capacitive coupling approximation.* From the literal solution we cannot only verify this concept but can also determine the specific restrictions on its applicability. We will also obtain the literal solution for time-domain analysis. From this solution we can immediately see the appropriate restrictions on the applicability of various approximate techniques that are outlined in various handbooks. Although these approximate techniques are simpler than a full solution of the MTL equations, it is important to know the limitations on their applicability.

The general statement of the problem is illustrated in Fig. 6.1(a). The line consists of three perfect conductors immersed in a lossless, homogeneous medium characterized by permittivity ε and permeability μ. The *generator circuit* is composed of a generator conductor with the reference conductor. It

is driven at the left end with an open-circuit source voltage, $V_S(t)$, and source resistance, R_S, and is terminated at the right end in a load resistance, R_L. The *receptor circuit* is composed of a receptor conductor and the reference conductor. It is terminated at the left or "near end" in a resistance, R_{NE}, and at the right or "far end" in a resistance, R_{FE}. Although resistive terminations are used in the following developments the frequency-domain phasor crosstalk results apply to complex-valued terminal impedances. The per-unit-length equivalent circuit is shown in Fig. 6.1(b). From this, the MTL equations can be derived in the usual manner and become

$$\frac{\partial}{\partial z}\mathbf{V}(z,t) = -\mathbf{L}\frac{\partial}{\partial t}\mathbf{I}(z,t) \tag{6.1a}$$

$$\frac{\partial}{\partial z}\mathbf{I}(z,t) = -\mathbf{C}\frac{\partial}{\partial t}\mathbf{V}(z,t) \tag{6.1b}$$

where

$$\mathbf{V}(z,t) = \begin{bmatrix} V_G(z,t) \\ V_R(z,t) \end{bmatrix} \tag{6.2a}$$

$$\mathbf{I}(z,t) = \begin{bmatrix} I_G(z,t) \\ I_R(z,t) \end{bmatrix} \tag{6.2b}$$

$$\mathbf{L} = \begin{bmatrix} l_G & l_m \\ l_m & l_R \end{bmatrix} \tag{6.2c}$$

$$\mathbf{C} = \begin{bmatrix} c_G + c_m & -c_m \\ -c_m & c_R + c_m \end{bmatrix} \tag{6.2d}$$

Subscript G denotes quantities associated with the generator circuit, whereas subscript R denotes quantities associated with the receptor circuit. Because of the assumption of a *homogeneous surrounding medium*, we have the important identity

$$\mathbf{LC} = \mu\varepsilon\mathbf{1}_2 = \frac{1}{v^2}\mathbf{1}_2 \tag{6.3}$$

where $v = 1/\sqrt{\mu\varepsilon}$ is the velocity of propagation of the waves in the medium. This identity gives the following relations between the per-unit-length parameters:

$$l_G(c_G + c_m) = l_R(c_R + c_m) \tag{6.4a}$$

$$l_m(c_G + c_m) = l_R c_m \tag{6.4b}$$

$$l_m(c_R + c_m) = l_G c_m \tag{6.4c}$$

The terminal conditions are written in the form of generalized Thévenin

equivalent characterizations as

$$\mathbf{V}(0, t) = \mathbf{V}_S(t) - \mathbf{R}_S\mathbf{I}(0, t) \tag{6.5a}$$

$$\mathbf{V}(\mathscr{L}, t) = \mathbf{R}_L\mathbf{I}(\mathscr{L}, t) \tag{6.5b}$$

where

$$\mathbf{V}_S(t) = \begin{bmatrix} V_S(t) \\ 0 \end{bmatrix} \tag{6.6a}$$

$$\mathbf{R}_S = \begin{bmatrix} R_S & 0 \\ 0 & R_{NE} \end{bmatrix} \tag{6.6b}$$

$$\mathbf{R}_L = \begin{bmatrix} R_L & 0 \\ 0 & R_{FE} \end{bmatrix} \tag{6.6c}$$

The objective is to obtain equations for the near-end and far-end crosstalk voltages; $V_{NE}(t) = V_R(0, t)$ and $V_{FE}(t) = V_R(\mathscr{L}, t)$.

6.1 FREQUENCY-DOMAIN SOLUTION

The MTL equations for sinusoidal steady-state excitation become

$$\frac{d}{dz}\hat{\mathbf{V}}(z) = -j\omega\mathbf{L}\hat{\mathbf{I}}(z) \tag{6.7a}$$

$$\frac{d}{dz}\hat{\mathbf{I}}(z) = -j\omega\mathbf{C}\hat{\mathbf{V}}(z) \tag{6.7b}$$

where the *phasor* line voltages and currents are

$$\hat{\mathbf{V}}(z) = \begin{bmatrix} \hat{V}_G(z) \\ \hat{V}_R(z) \end{bmatrix} \tag{6.8a}$$

$$\hat{\mathbf{I}}(z) = \begin{bmatrix} \hat{I}_G(z) \\ \hat{I}_R(z) \end{bmatrix} \tag{6.8b}$$

The phasor generalized Thévenin equivalent characterization of the terminations becomes

$$\hat{\mathbf{V}}(0) = \hat{\mathbf{V}}_S - \mathbf{R}_S\hat{\mathbf{I}}(0) \tag{6.9a}$$

$$\hat{\mathbf{V}}(\mathscr{L}) = \mathbf{R}_L\hat{\mathbf{I}}(\mathscr{L}) \tag{6.9b}$$

where

$$\hat{\mathbf{V}}_S = \begin{bmatrix} \hat{V}_S \\ 0 \end{bmatrix} \tag{6.10a}$$

$$\mathbf{R}_S = \begin{bmatrix} R_S & 0 \\ 0 & R_{NE} \end{bmatrix} \tag{6.10b}$$

$$\mathbf{R}_L = \begin{bmatrix} R_L & 0 \\ 0 & R_{FE} \end{bmatrix} \tag{6.10c}$$

The objective is to obtain equations for the phasor near-end and far-end crosstalk voltages; $\hat{V}_{NE} = \hat{V}_R(0)$ and $\hat{V}_{FE} = \hat{V}_R(\mathscr{L})$.

The chain parameter matrix was derived for this case in Chapter 4 and becomes

$$\begin{bmatrix} \hat{\mathbf{V}}(\mathscr{L}) \\ \hat{\mathbf{I}}(\mathscr{L}) \end{bmatrix} = \begin{bmatrix} \hat{\Phi}_{11} & \hat{\Phi}_{12} \\ \hat{\Phi}_{21} & \hat{\Phi}_{22} \end{bmatrix} \begin{bmatrix} \hat{\mathbf{V}}(0) \\ \hat{\mathbf{I}}(0) \end{bmatrix} \tag{6.11}$$

The chain parameter submatrices simplify for this case of perfect conductors in a lossless, homogeneous medium to

$$\hat{\Phi}_{11} = C\mathbf{1}_2 \tag{6.12a}$$

$$\hat{\Phi}_{12} = -j\omega\mathscr{L}S\mathbf{L} \tag{6.12b}$$

$$\hat{\Phi}_{21} = -j\omega\mathscr{L}S\mathbf{C} \tag{6.12c}$$

$$\hat{\Phi}_{22} = C\mathbf{1}_2 \tag{6.12d}$$

where

$$C = \cos(\beta\mathscr{L}) \tag{6.13a}$$

$$S = \frac{\sin(\beta\mathscr{L})}{\beta\mathscr{L}} \tag{6.13b}$$

The velocity of propagation is

$$v = \frac{1}{\sqrt{\mu\varepsilon}} \tag{6.14a}$$

and the phase constant is

$$\beta = \frac{\omega}{v} \tag{6.14b}$$

The terminal characterization in (6.9) is substituted into the chain parameter matrix in (6.11) to give

$$(\hat{\Phi}_{11}\mathbf{R}_S + \mathbf{R}_L\hat{\Phi}_{22} - \hat{\Phi}_{12} - \mathbf{R}_L\hat{\Phi}_{21}\mathbf{R}_S)\hat{\mathbf{I}}(0) = (\hat{\Phi}_{11} - \mathbf{R}_L\hat{\Phi}_{21})\hat{\mathbf{V}}_S \tag{6.15a}$$

$$(\hat{\Phi}_{11}\mathbf{R}_L + \mathbf{R}_S\hat{\Phi}_{22} - \hat{\Phi}_{12} - \mathbf{R}_S\hat{\Phi}_{21}\mathbf{R}_L)\hat{\mathbf{I}}(\mathscr{L}) = \hat{\mathbf{V}}_S \tag{6.15b}$$

Substituting the chain parameter submatrices given in (6.12) into (6.15) gives

$$\left[\cos(\beta\mathscr{L})(\mathbf{R}_S+\mathbf{R}_L)+\frac{\sin(\beta\mathscr{L})}{\beta\mathscr{L}}(\mathbf{R}_L j\omega\mathbf{C}\mathscr{L}\mathbf{R}_S+j\omega\mathbf{L})\right]\hat{\mathbf{I}}(0) \tag{6.16a}$$

$$=\left[\cos(\beta\mathscr{L})\mathbf{1}_2+\frac{\sin(\beta\mathscr{L})}{\beta\mathscr{L}}\mathbf{R}_L j\omega\mathbf{C}\mathscr{L}\right]\hat{\mathbf{V}}_S$$

$$\left[\cos(\beta\mathscr{L})(\mathbf{R}_S+\mathbf{R}_L)+\frac{\sin(\beta\mathscr{L})}{\beta\mathscr{L}}(\mathbf{R}_S j\omega\mathbf{C}\mathscr{L}\mathbf{R}_L+j\omega\mathbf{L})\right]\hat{\mathbf{I}}(\mathscr{L})=\hat{\mathbf{V}}_S \tag{6.16b}$$

Once these are solved, the near-end and far-end crosstalk voltages are obtained from the second entries in these solution vectors as $\hat{V}_{NE}=\hat{V}_R(0)=-R_{NE}\hat{I}_R(0)$ and $\hat{V}_{FE}=\hat{V}_R(\mathscr{L})=R_{FE}\hat{I}_R(\mathscr{L})$.

Equations (6.16) were solved in [B.5] via Cramer's rule in literal form to yield the following *exact* literal solution for the crosstalk voltages:

$$\hat{V}_{NE}=\frac{S}{Den}[j\omega M_{NE}C+(j\omega)^2TK_{NE}S]\hat{V}_S \tag{6.17a}$$

$$\hat{V}_{FE}=\frac{S}{Den}(j\omega M_{FE})\hat{V}_S \tag{6.17b}$$

$$Den=C^2+(j\omega)^2S^2\tau_G\tau_R P+j\omega CS(\tau_G+\tau_R) \tag{6.17c}$$

The various quantities in these equations are [B.5]

$$M_{NE}=M_{NE}^{IND}+M_{NE}^{CAP} \tag{6.18a}$$

$$M_{FE}=M_{FE}^{IND}+M_{FE}^{CAP} \tag{6.18b}$$

where the *inductive-coupling* coefficients are

$$M_{NE}^{IND}=\frac{R_{NE}}{R_{NE}+R_{FE}}l_m\mathscr{L}\frac{1}{R_S+R_L} \tag{6.19a}$$

$$M_{FE}^{IND}=-\frac{R_{FE}}{R_{NE}+R_{FE}}l_m\mathscr{L}\frac{1}{R_S+R_L} \tag{6.19b}$$

and the *capacitive-coupling* coefficients are

$$M_{NE}^{CAP}=\frac{R_{NE}R_{FE}}{R_{NE}+R_{FE}}c_m\mathscr{L}\frac{R_L}{R_S+R_L} \tag{6.20a}$$

$$M_{FE}^{CAP}=M_{NE}^{CAP} \tag{6.20b}$$

The remaining quantities are defined in the following way. The coefficient K_{NE} is defined by

$$K_{NE} = M_{NE}^{IND} \frac{1}{\sqrt{1-k^2}} \alpha_{LG} + M_{NE}^{CAP} \frac{1}{\sqrt{1-k^2}} \frac{1}{\alpha_{LG}} \tag{6.21}$$

The coupling coefficient between the two circuits is defined by

$$k = \frac{l_m}{\sqrt{l_G l_R}} \tag{6.22}$$

and the circuit characteristic impedances are defined by

$$Z_{CG} = v l_G \sqrt{1-k^2} \tag{6.23a}$$

$$Z_{CR} = v l_R \sqrt{1-k^2} \tag{6.23b}$$

The line one-way delay is denoted by

$$T = \frac{\mathscr{L}}{v} \tag{6.24}$$

The relationships of the termination impedances to the characteristic impedances are important parameters. In order to highlight this dependency, the various ratios of termination impedance to characteristic impedance are defined by

$$\left.\begin{aligned} \alpha_{SG} &= \frac{R_S}{Z_{CG}} \quad \alpha_{LG} = \frac{R_L}{Z_{CG}} \\ \alpha_{SR} &= \frac{R_{NE}}{Z_{CR}} \quad \alpha_{LR} = \frac{R_{FE}}{Z_{CR}} \end{aligned}\right\} \tag{6.25}$$

In terms of these ratios, the factor P in *Den* becomes

$$P = \left[1 - k^2 \frac{(1-\alpha_{SG}\alpha_{LR})(1-\alpha_{LG}\alpha_{SR})}{(1+\alpha_{SG}\alpha_{LG})(1+\alpha_{SR}\alpha_{LR})}\right] \tag{6.26}$$

Observe that $P = 1$ if the line is *weakly coupled*, $k \ll 1$, and/or the lines are matched at opposite ends, $\alpha_{SG} = \alpha_{LR} = 1$, or $\alpha_{SR} = \alpha_{LG} = 1$. The circuit *time*

constants are logically defined as

$$\tau_G = \frac{l_G \mathscr{L}}{R_S + R_L} + (c_G + c_m)\mathscr{L}\frac{R_S R_L}{R_S + R_L} \tag{6.27a}$$

$$= \frac{T}{\sqrt{1-k^2}}\left\{\frac{1 + \alpha_{SG}\alpha_{LG}}{\alpha_{SG} + \alpha_{LG}}\right\}$$

$$\tau_R = \frac{l_R \mathscr{L}}{R_{NE} + R_{FE}} + (c_R + c_m)\mathscr{L}\frac{R_{NE} R_{FE}}{R_{NE} + R_{FE}} \tag{6.27b}$$

$$= \frac{T}{\sqrt{1-k^2}}\left\{\frac{1 + \alpha_{SR}\alpha_{LR}}{\alpha_{SR} + \alpha_{LR}}\right\}$$

Observe that a line time constant is equal to the line one-way delay if the lines are weakly coupled, $k \ll 1$, and that line is matched at one end. In other words, $\tau_l = T$ if $k \ll 1$ and $\alpha_{Sl} = 1$ or $\alpha_{Ll} = 1$.

6.1.1 Inductive and Capacitive Coupling

The above results are an exact literal solution for the problem. No assumptions about symmetry or matched loads are used. Therefore they cover a wider class of problems than have been considered in the past. Although they have been simplified by defining certain terms, they can be simplified further if we make the following assumptions. First let us assume that *the line is electrically short at the frequency of interest*, i.e., $\mathscr{L} \ll \lambda$. In this case the terms C and S simplify to

$$C = \cos(\beta\mathscr{L}) \tag{6.28a}$$

$$= \cos\left(2\pi\frac{\mathscr{L}}{\lambda}\right)$$

$$\cong 1$$

$$S = \frac{\sin(\beta\mathscr{L})}{\beta\mathscr{L}} \tag{6.28b}$$

$$\cong 1$$

Further let us assume that *the line is weakly coupled*, i.e., $k \ll 1$. Under these assumptions, there exists a sufficiently small frequency such that the exact results in (6.17) simplify to

$$\hat{V}_{NE} \cong j\omega\left(\underbrace{\frac{R_{NE}}{R_{NE} + R_{FE}} l_m \mathscr{L}\frac{1}{R_S + R_L}}_{M_{NE}^{IND}} + \underbrace{\frac{R_{NE} R_{FE}}{R_{NE} + R_{FE}} c_m \mathscr{L}\frac{R_L}{R_S + R_L}}_{M_{NE}^{CAP}}\right)\hat{V}_S \tag{6.29a}$$

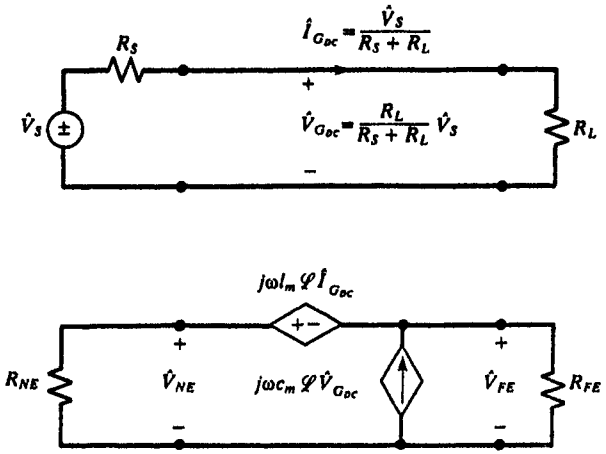

FIGURE 6.2 The frequency-domain inductive-capacitive low-frequency coupling model.

$$\hat{V}_{FE} \cong j\omega \left(\underbrace{-\frac{R_{FE}}{R_{NE}+R_{FE}} l_m \mathscr{L} \frac{1}{R_S+R_L}}_{M_{FE}^{IND}} + \underbrace{\frac{R_{NE}R_{FE}}{R_{NE}+R_{FE}} c_m \mathscr{L} \frac{R_L}{R_S+R_L}}_{M_{FE}^{CAP}} \right) \hat{V}_S \quad (6.29b)$$

These low-frequency results can be computed from the equivalent circuit of Fig. 6.2. The terms depending on the per-unit-length mutual inductance l_m are referred to as the *inductive coupling contributions*, whereas the terms depending on the per-unit-length mutual capacitance c_m are referred to as the *capacitive coupling contributions*.

Observe that the low-frequency, weakly coupled approximate results in (6.29) show that the crosstalk varies directly with frequency or 20 dB/decade and the total coupling can be written as the sum of inductive-coupling and capacitive-coupling components as

$$\hat{V}_{NE} \cong \hat{V}_{NE}^{IND} + \hat{V}_{NE}^{CAP} \quad (6.30a)$$
$$= j\omega M_{NE}^{IND} \hat{V}_S + j\omega M_{NE}^{CAP} \hat{V}_S$$
$$\hat{V}_{FE} \cong \hat{V}_{FE}^{IND} + \hat{V}_{FE}^{CAP} \quad (6.30b)$$
$$= j\omega M_{FE}^{IND} \hat{V}_S + j\omega M_{FE}^{CAP} \hat{V}_S$$

where

$$M_{NE}^{IND} = \frac{R_{NE}}{R_{NE}+R_{FE}} l_m \mathscr{L} \frac{1}{R_S+R_L} \quad (6.31a)$$

$$M_{FE}^{IND} = -\frac{R_{FE}}{R_{NE}+R_{FE}} l_m \mathscr{L} \frac{1}{R_S+R_L} \quad (6.31b)$$

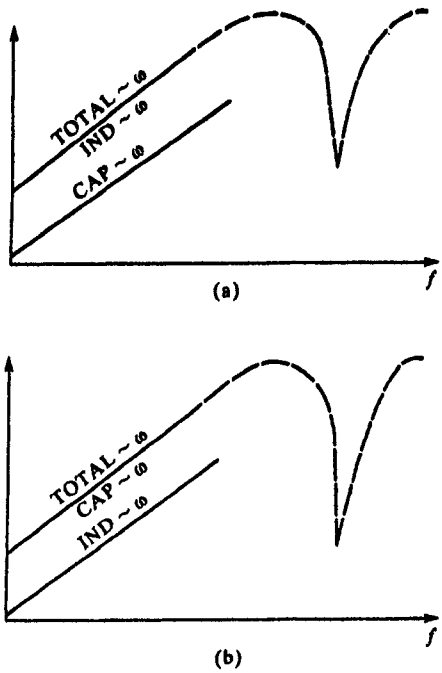

FIGURE 6.3 Illustration of the dominance of inductive (capacitive) coupling for (a) low- and (b) high-impedance terminations.

$$M_{NE}^{CAP} = M_{FE}^{CAP} = \frac{R_{NE}R_{FE}}{R_{NE} + R_{FE}} c_m \mathscr{L} \frac{R_L}{R_S + R_L} \tag{6.31c}$$

Depending on the levels of the load impedances, the inductive-coupling contribution may dominate the capacitive-coupling contribution or vice versa. This is illustrated in Fig. 6.3. If the termination impedances are much smaller than the line characteristic impedances, i.e., *low-impedance loads*, then inductive coupling dominates. On the other hand, capacitive coupling dominates in the case of *high-impedance loads*. Although this approximation is valid only for weakly coupled lines and for a sufficiently small frequency where the line is electrically short, this separation of the total coupling into an inductive-coupling and a capacitive-coupling component provides considerable understanding of crosstalk phenomena. In particular, it readily explains how shields and/or twisted pairs of wires may or may not reduce crosstalk [A.3].

6.1.2 Common-Impedance Coupling

The above derivation assumes that all three conductors are *perfect conductors* and the surrounding homogeneous medium is *lossless*. Losses can be ignored

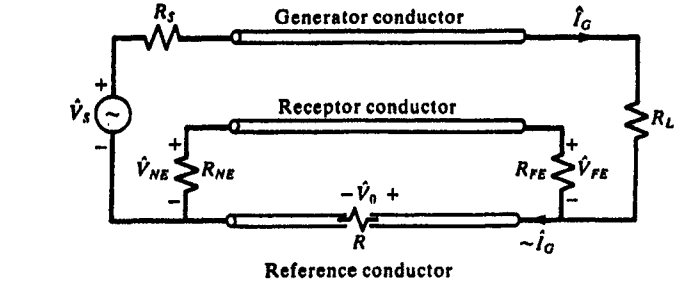

(a)

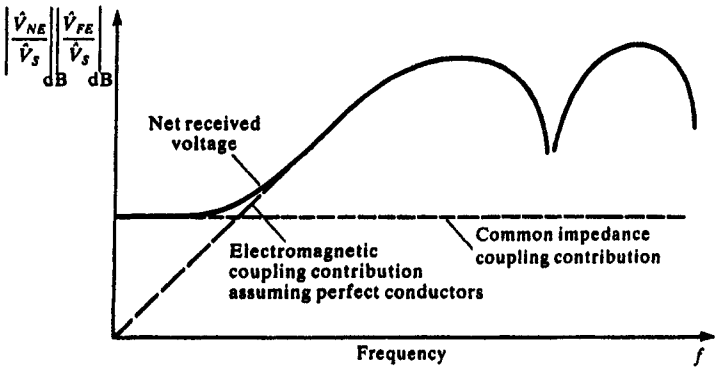

(b)

FIGURE 6.4 Illustration of common-impedance coupling due to a lossy reference conductor.

in many practical problems. However, there is a potentially significant contribution to crosstalk via imperfect conductors that occurs at the lower frequencies. This is referred to as *common-impedance coupling* and is contributed by the impedance of the reference conductor.

Figure 6.4 illustrates the problem. As the frequency of excitation is lowered, the crosstalk decreases directly with frequency. At some lower frequency, this contribution due to the electric and magnetic field interaction between the two circuits is dominated by the *common-impedance coupling component.* At a sufficiently low frequency, the current in the generator circuit, $\hat{I}_G$, returns predominantly in the reference conductor and can be computed from

$$\hat{I}_G \cong \frac{1}{R_S + R_L}\hat{V}_S \tag{6.32}$$

If we lump the per-unit-length resistance of the reference conductor, r, as a total

resistance, $R = r\mathscr{L}$, then a voltage drop of

$$\hat{V}_0 = r\mathscr{L}\hat{I}_G = \frac{r\mathscr{L}}{R_S + R_L}\hat{V}_S \tag{6.33}$$

is developed across the reference conductor. This is voltage-divided across the termination resistors of the receptor circuit to give

$$\hat{V}_{NE}^{CI} = \underbrace{\frac{R_{NE}}{R_{NE} + R_{FE}} r\mathscr{L} \frac{1}{R_S + R_L}}_{M_{NE}^{CI}} \hat{V}_S \tag{6.34a}$$

$$\hat{V}_{FE}^{CI} = -\underbrace{\frac{R_{FE}}{R_{NE} + R_{FE}} r\mathscr{L} \frac{1}{R_S + R_L}}_{M_{FE}^{CI}} \hat{V}_S \tag{6.34b}$$

In an approximate sense, we may simply combine these contributions with the inductive-capacitive coupling contributions in (6.30) to give the total as

$$\begin{aligned}\hat{V}_{NE} &\cong \hat{V}_{NE}^{IND} + \hat{V}_{NE}^{CAP} + \hat{V}_{NE}^{CI} \\ &= j\omega M_{NE}^{IND}\hat{V}_S + j\omega M_{NE}^{CAP}\hat{V}_S + M_{NE}^{CI}\hat{V}_S\end{aligned} \tag{6.35a}$$

$$\begin{aligned}\hat{V}_{FE} &\cong \hat{V}_{FE}^{IND} + \hat{V}_{FE}^{CAP} + \hat{V}_{FE}^{CI} \\ &= j\omega M_{FE}^{IND}\hat{V}_S + j\omega M_{FE}^{CAP}\hat{V}_S + M_{FE}^{CI}\hat{V}_S\end{aligned} \tag{6.35b}$$

This approximate inclusion of the impedance of the reference conductor at low frequencies was verified in [B.14] by deriving the exact chain parameter matrix with the per-unit-length resistance of the reference conductor included.

6.2 TIME-DOMAIN SOLUTION

To obtain the exact time-domain solution we will assume $V_S(t) = 0$ for $t \leq 0$ and the line is initially relaxed: $\mathbf{V}(z, t) = \mathbf{I}(z, t) = \mathbf{0}$ for all $0 \leq z \leq \mathscr{L}$ and $t \leq 0$ [B.15]. In this case the Laplace transform variable s can be substituted for $j\omega$ in the above frequency-domain exact solution. Substituting $j\omega \rightarrow s$ in (6.13) gives

$$j\omega S = j\omega \frac{\sin\left(\frac{\omega\mathscr{L}}{v}\right)}{\frac{\omega\mathscr{L}}{v}} \Rightarrow \frac{e^{sT} - e^{-sT}}{2T} \tag{6.36a}$$

$$C = \cos\left(\frac{\omega\mathscr{L}}{v}\right) \Rightarrow \frac{e^{sT} + e^{-sT}}{2} \tag{6.36b}$$

where the line one-way time delay is

$$T = \frac{\mathscr{L}}{v} \tag{6.37}$$

Substituting these along with $j\omega \to s$ into (6.17) gives the *exact* Laplace-transformed time-domain solution:

$$V_{NE}(s) = \frac{T}{X}\frac{(M_{NE} + K_{NE}) - 2K_{NE}e^{-2sT} + (K_{NE} - M_{NE})e^{-4sT}}{1 + ae^{-2sT} + be^{-4sT}} V_S(s) \tag{6.38a}$$

$$V_{FE}(s) = 2\frac{T}{X}\frac{M_{NE}(e^{-sT} - e^{-3sT})}{1 + ae^{-2sT} + be^{-4sT}} V_S(s) \tag{6.38b}$$

where

$$X = [T^2 + \tau_G\tau_R P + T(\tau_G + \tau_R)] \tag{6.39a}$$

$$a = \frac{2(T^2 - \tau_G\tau_R P)}{T^2 + \tau_G\tau_R P + T(\tau_G + \tau_R)} \tag{6.39b}$$

$$b = \frac{T^2 + \tau_G\tau_R P - T(\tau_G + \tau_R)}{T^2 + \tau_G\tau_R P + T(\tau_G + \tau_R)} \tag{6.39c}$$

where $V_S(s)$ is the Laplace transform of $V_S(t)$.

We now take the inverse Laplace transform of these results. Rewrite (6.38a) and (6.38b) as

$$(1 + ae^{-2sT} + be^{-4sT})V_{NE}(s) \tag{6.40a}$$

$$= \frac{T}{X}[(M_{NE} + K_{NE}) - 2K_{NE}e^{-2sT} + (K_{NE} - M_{NE})e^{-4sT}]V_S(s)$$

$$(1 + ae^{-2sT} + be^{-4sT})V_{FE}(s) = 2\frac{T}{X}M_{NE}(e^{-sT} - e^{-3sT})V_S(s) \tag{6.40b}$$

In taking the inverse Laplace transform of this result we recall the simple time-delay transform pair:

$$F(t \pm nT) \leftrightarrow e^{\pm nsT}F(s) \tag{6.41}$$

Therefore the exact time-domain expressions become

$$V_{NE}(t) = -aV_{NE}(t-2T) - bV_{NE}(t-4T) + \frac{T}{X}(M_{NE}+K_{NE})V_S(t) \qquad (6.42a)$$

$$-2\frac{T}{X}K_{NE}V_S(t-2T) + \frac{T}{X}(K_{NE}-M_{NE})V_S(t-4T)$$

$$V_{FE}(t) = -aV_{FE}(t-2T) - bV_{FE}(t-4T) + 2\frac{T}{X}M_{NE}[V_S(t-T) - V_S(t-3T)] \qquad (6.42b)$$

These equations can be solved recursively for the crosstalk voltages realizing that $V_S(t) = V_{NE}(t) = V_{FE}(t) = 0$ for $t \leq 0$. The solutions are in terms of values of the source voltage at the present time, $V_S(t)$; at various time delays prior to the present time, $V_S(t-T)$, $V_S(t-2T)$, $V_S(t-3T)$, and $V_S(t-4T)$; as well as prior solutions at various time delays prior to the present time, $V_{NE}(t-2T)$, $V_{NE}(t-4T)$, $V_{FE}(t-2T)$, and $V_{FE}(t-4T)$.

6.2.1 Explicit Solution

Although the solution in (6.42) is exact, it requires knowledge of the solution at previous times that are multiples of the line one-way delay, T. Thus a recursive solution is required. In order to obtain a solution that depends only on $V_S(t)$ we introduce the *time-shift* or *difference operator*, D, where

$$D^m F(t) \equiv F(t+mT) \qquad (6.43a)$$

$$D^{-m}F(t) \equiv F(t-mT) \qquad (6.43b)$$

Using the time-shift operator in (6.40) gives

$$(1 + aD^{-2} + bD^{-4})V_{NE}(t) \qquad (6.44a)$$

$$= \frac{T}{X}[(M_{NE}+K_{NE}) - 2K_{NE}D^{-2} + (K_{NE}-M_{NE})D^{-4}]V_S(t)$$

$$(1 + aD^{-2} + bD^{-4})V_{FE}(t) = 2\frac{T}{X}M_{NE}(D^{-1} - D^{-3})V_S(t) \qquad (6.44b)$$

Multiplying the equations by powers of D gives the transfer functions in terms of the time-shift operator, D, as

$$V_{NE}(t) = \frac{T}{X}\frac{(M_{NE}+K_{NE})D^4 - 2K_{NE}D^2 + (K_{NE}-M_{NE})}{D^4 + aD^2 + b}V_S(t) \qquad (6.45a)$$

$$= \frac{T}{X}\frac{M_{NE}(D^4-1) + K_{NE}(D^4 - 2D^2 + 1)}{D^4 + aD^2 + b}V_S(t)$$

$$V_{FE}(t) = 2\frac{T}{X} M_{NE} \frac{D^3 - D}{D^4 + aD^2 + b} V_S(t) \tag{6.45b}$$

These expressions can be inverted by carrying out the long division of the following basic problem:

$$\frac{1}{D^4 + aD^2 + b} = \alpha_0 D^{-4} + \alpha_1 D^{-6} + \alpha_2 D^{-8} + \alpha_3 D^{-10} + \alpha_4 D^{-12} \tag{6.46a}$$
$$+ \alpha_5 D^{-14} + \alpha_6 D^{-16} + \cdots$$

where

$$\begin{aligned} \alpha_0 &= 1 \\ \alpha_1 &= -a \\ \alpha_2 &= a^2 - b \\ \alpha_3 &= -a^3 + 2ab \\ \alpha_4 &= a^4 - 3a^2 b + b^2 \\ \alpha_5 &= -a^5 + 4a^3 b - 3ab^2 \\ \alpha_6 &= a^6 - 5a^4 b + 6a^2 b^2 - b^3 \\ &\vdots \end{aligned} \tag{6.46b}$$

Substituting the results in (6.46) into (6.45) gives the time-domain crosstalk voltages in terms of $V_S(t)$ delayed by multiples of the one-way line delay, T, as

$$V_{NE}(t) = N_0 V_S(t) + N_2 V_S(t - 2T) + N_4 V_S(t - 4T) \tag{6.47a}$$
$$+ N_6 V_S(t - 6T) + \cdots$$
$$V_{FE}(t) = F_1 V_S(t - T) + F_3 V_S(t - 3T) + F_5 V_S(t - 5T) \tag{6.47b}$$
$$+ F_7 V_S(t - 7T) + \cdots$$

where the constants are

$$\left.\begin{aligned} N_0 &= \frac{T}{X}[M_{NE}(\alpha_0) + K_{NE}(\alpha_0)] \\ N_2 &= \frac{T}{X}[M_{NE}(\alpha_1) + K_{NE}(\alpha_1 - 2\alpha_0)] \\ N_4 &= \frac{T}{X}[M_{NE}(\alpha_2 - \alpha_0) + K_{NE}(\alpha_2 - 2\alpha_1 + \alpha_0)] \\ N_6 &= \frac{T}{X}[M_{NE}(\alpha_3 - \alpha_1) + K_{NE}(\alpha_3 - 2\alpha_2 + \alpha_1)] \\ N_8 &= \frac{T}{X}[M_{NE}(\alpha_4 - \alpha_2) + K_{NE}(\alpha_4 - 2\alpha_3 + \alpha_2)] \\ N_{10} &= \frac{T}{X}[M_{NE}(\alpha_5 - \alpha_3) + K_{NE}(\alpha_5 - 2\alpha_4 + \alpha_3)] \end{aligned}\right\} \tag{6.48a}$$

and

$$\left.\begin{aligned} F_1 &= 2\frac{T}{X} M_{FE}(\alpha_0) \\ F_3 &= 2\frac{T}{X} M_{FE}(\alpha_1 - \alpha_0) \\ F_5 &= 2\frac{T}{X} M_{FE}(\alpha_2 - \alpha_1) \\ F_7 &= 2\frac{T}{X} M_{FE}(\alpha_3 - \alpha_2) \\ F_9 &= 2\frac{T}{X} M_{FE}(\alpha_4 - \alpha_3) \\ F_{11} &= 2\frac{T}{X} M_{FE}(\alpha_5 - \alpha_4) \\ &\vdots \end{aligned}\right\} \tag{6.48b}$$

These final expressions give the explicit relationships for the crosstalk voltages as linear combinations of the source voltage delayed in time by various multiples of the line one-way delay, T.

6.2.2 Weakly Coupled Lines

The above time-domain solutions are exact but somewhat complicated. Quite often the lines can be considered to be *weakly coupled*, $k \ll 1$. This assumption simplifies the above exact results. For a weakly coupled line, the factor P in (6.26) approximates to unity, $P \cong 1$, and the characteristic impedances approximate to $Z_{CG} \cong vl_G$, $Z_{CR} \cong vl_R$. The quantities in (6.39) approximate to

$$X = (T + \tau_G)(T + \tau_R) \tag{6.49a}$$

$$a = \frac{(T - \tau_G)}{(T + \tau_G)} + \frac{(T - \tau_R)}{(T + \tau_R)} \tag{6.49b}$$

$$b = \frac{(T - \tau_G)}{(T + \tau_G)} \frac{(T - \tau_R)}{(T + \tau_R)} \tag{6.49c}$$

Substituting the time constants in terms of the ratios of the termination resistances to the line characteristic impedances given in (6.27) gives

$$X = T^2\left[\frac{(1 + \alpha_{SG})(1 + \alpha_{LG})(1 + \alpha_{SR})(1 + \alpha_{LR})}{(\alpha_{SG} + \alpha_{LG})(\alpha_{SR} + \alpha_{LR})}\right] \tag{6.50a}$$

$$a = -(\Gamma_{SG}\Gamma_{LG} + \Gamma_{SR}\Gamma_{LR}) \tag{6.50b}$$

$$b = \Gamma_{SG}\Gamma_{LG}\Gamma_{SR}\Gamma_{LR} \tag{6.50c}$$

where the reflection coefficients are logically defined as

$$\Gamma_{SG} = \frac{(R_S - Z_{CG})}{(R_S + Z_{CG})} = \frac{(\alpha_{SG} - 1)}{(\alpha_{SG} + 1)} \tag{6.51a}$$

$$\Gamma_{LG} = \frac{(R_L - Z_{CG})}{(R_L + Z_{CG})} = \frac{(\alpha_{LG} - 1)}{(\alpha_{LG} + 1)} \tag{6.51b}$$

$$\Gamma_{SR} = \frac{(R_{NE} - Z_{CR})}{(R_{NE} + Z_{CR})} = \frac{(\alpha_{SR} - 1)}{(\alpha_{SR} + 1)} \tag{6.51c}$$

$$\Gamma_{LR} = \frac{(R_{FE} - Z_{CR})}{(R_{FE} + Z_{CR})} = \frac{(\alpha_{LR} - 1)}{(\alpha_{LR} + 1)} \tag{6.51d}$$

If we define the quantities

$$K_G = \Gamma_{SG}\Gamma_{LG} \tag{6.52a}$$

$$K_R = \Gamma_{SR}\Gamma_{LR} \tag{6.52b}$$

then the quantities in (6.46b) become

$$\begin{aligned}
\alpha_0 &= 1 \\
\alpha_2 &= K_G + K_G K_R + K_R^2 \\
\alpha_3 &= K_G^3 + K_G^2 K_R + K_G K_R^2 + K_R^3 \\
\alpha_4 &= K_G^4 + K_G^3 K_R + K_G^2 K_R^2 + K_G K_R^3 + K_R^4 \\
\alpha_5 &= K_G^5 + K_G^4 K_R + K_G^3 K_R^2 + K_G^2 K_R^3 + K_G K_R^4 + K_R^5 \\
&\vdots
\end{aligned} \tag{6.53}$$

Suppose that the line is weakly coupled and the generator circuit is matched at one end, $\Gamma_{SG} = 0$ or $\Gamma_{LG} = 0$. In this case $K_G = 0$ so that $\alpha_0 = 1$, $\alpha_1 = K_R = \Gamma_{SR}\Gamma_{LR}$, $\alpha_2 = K_R^2 = \Gamma_{SR}^2\Gamma_{LR}^2$, $\alpha_3 = K_R^3 = \Gamma_{SR}^3\Gamma_{LR}^3, \ldots$. Alternatively, suppose that the line is weakly coupled and the receptor circuit is matched at one end, $\Gamma_{SR} = 0$ or $\Gamma_{LR} = 0$. In this case, $K_R = 0$ so that $\alpha_0 = 1$, $\alpha_1 = K_G = \Gamma_{SG}\Gamma_{LG}$, $\alpha_2 = K_G^2 = \Gamma_{SG}^2\Gamma_{LG}^2$, $\alpha_3 = K_G^3 = \Gamma_{SG}^3\Gamma_{LG}^3, \ldots$. For either of these cases the results in (6.47) simplify somewhat.

Now suppose that the line is weakly coupled and that one of the ends of *each* line is matched; $\Gamma_{SG} = 0$ or $\Gamma_{LG} = 0$ *and* $\Gamma_{SR} = 0$ or $\Gamma_{LR} = 0$. In this case, $\tau_G = T$ and $\tau_R = T$ so that $X = 4T^2$. The quantities K_G and K_R in (6.52) are zero so that $\alpha_1 = \alpha_2 = \cdots = 0$. The near-end and far-end crosstalk expressions

in (6.47) simplify to

$$V_{NE}(t) = \frac{M_{NE}}{4T}[V_S(t) - V_S(t-4T)] \tag{6.54a}$$

$$+ \frac{K_{NE}}{4T}[V_S(t) - 2V_S(t-2T) + V_S(t-4T)]$$

$$V_{FE}(t) = \frac{M_{FE}}{2T}[V_S(t-T) - V_S(t-3T)] \tag{6.54b}$$

If the line happens to be matched at the load end of the generator circuit, $\Gamma_{LG} = 0$, then $K_{NE} = M_{NE}$ and (6.54) simplify to

$$V_{NE}(t) = \frac{M_{NE}}{2T}[V_S(t) - V_S(t-2T)] \tag{6.55a}$$

$$V_{FE}(t) = \frac{M_{FE}}{2T}[V_S(t-T) - V_S(t-3T)] \tag{6.55b}$$

There exist numerous electronic design handbooks and other publications that contain time-domain crosstalk prediction equations for three-conductor lines [5–11]. However, as pointed out previously, these invariably make the following assumptions:

1. The line is *weakly coupled.*
2. All ports are matched: $\Gamma_{SG} = \Gamma_{LG} = \Gamma_{SR} = \Gamma_{LR} = 0$.
3. Both circuits have identical cross sections, e.g., two identical wires at the same height about a ground plane.

These are very special restrictions that are generally not fulfilled in practical cases. Nevertheless, for a line that satisfies the above ideal conditions, the previously derived *exact* crosstalk results reduce to

$$V_{NE}(t) = \frac{\mathscr{L}}{8T}\left(\frac{l_m}{Z_C} + c_m Z_C\right)[V_S(t) - V_S(t-2T)] \tag{6.56a}$$

$$V_{FE}(t) = -\frac{\mathscr{L}}{8T}\left(\frac{l_m}{Z_C} - c_m Z_C\right)[V_S(t-T) - V_S(t-3T)] \tag{6.56b}$$

$$= 0$$

These results are equivalent to results derived intuitively in [5–7]. Observe that the far-end crosstalk is zero for this completely matched line in a homogeneous medium.

6.2.3 Inductive and Capacitive Coupling

In the frequency-domain solution we observed that for a weakly coupled, electrically short line and for a sufficiently small frequency, the near-end and far-end crosstalk voltages reduce to

$$\hat{V}_{NE}(j\omega) \cong j\omega M_{NE}\hat{V}_S(j\omega) \tag{6.57a}$$

$$\hat{V}_{FE}(j\omega) \cong j\omega M_{FE}\hat{V}_S(j\omega) \tag{6.57b}$$

The time-domain results can be obtained from these by substituting

$$j\omega \Rightarrow \frac{\mathrm{d}}{\mathrm{dt}} \tag{6.58}$$

to give

$$V_{NE}(t) \cong M_{NE}\frac{d}{dt}V_S(t) \tag{6.59a}$$

$$V_{FE}(t) \cong M_{FE}\frac{d}{dt}V_S(t) \tag{6.59b}$$

For trapezoidal pulses representing, perhaps, digital clock or data signals, these results give crosstalk pulses occurring during the transitions of $V_S(t)$ with the levels of those pulses dependent on the slope or "slew rate" of $V_S(t)$ as illustrated in Fig. 6.5. Substituting the definitions of M_{NE} and M_{FE} in terms of inductive- and capacitive-coupling contributions as given in (6.18) and (6.19) shows that this approximated time-domain crosstalk result can be computed from the equivalent circuit shown in Fig. 6.6. Therefore, the time-domain crosstalk is the sum of an inductive-coupling component and a capacitive-coupling component. This result can also be seen from the approximate result derived for a *completely matched, weakly coupled line* given in (6.55):

$$V_{NE}(t) = M_{NE}\frac{[V_S(t) - V_S(t-2T)]}{2T} \tag{6.60a}$$

$$V_{FE}(t) = M_{FE}\frac{[V_S(t-T) - V_S(t-3T)]}{2T} \tag{6.60b}$$

If the one-way delay is sufficiently small compared to the rise/fall times of the source voltage, i.e.,

$$\tau_r, \tau_f \gg T \tag{6.61}$$

the derivatives of the source voltage are reasonably approximated by

$$\frac{d}{dt}V_S(t) \cong \frac{[V_S(t) - V_S(t-2T)]}{2T} \tag{6.62a}$$

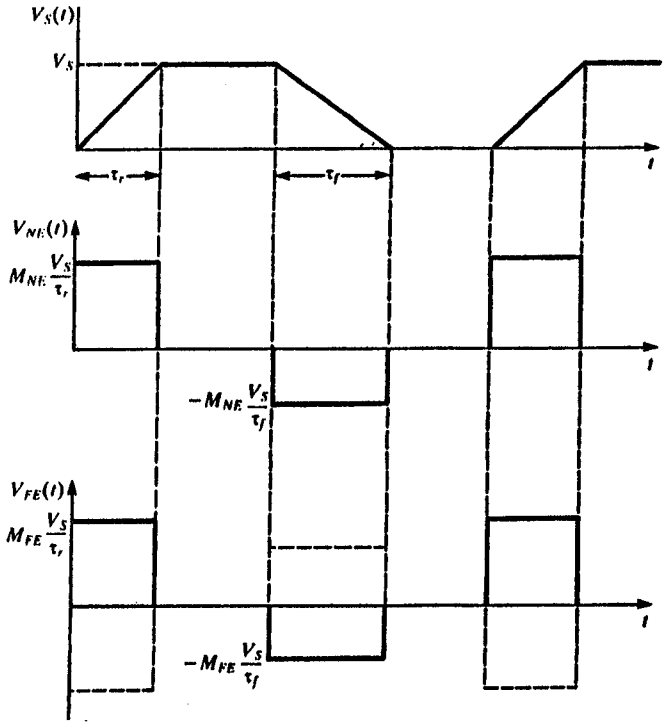

FIGURE 6.5 Illustration of near-end and far-end time-domain crosstalk predicted by the inductive-capacitive coupling model.

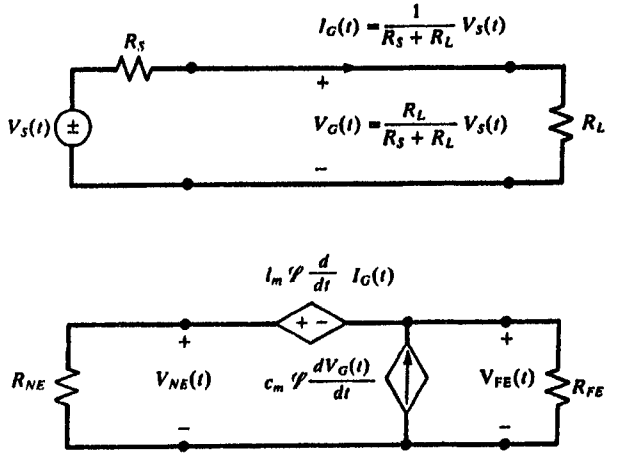

FIGURE 6.6 The time-domain inductive-capacitive coupling model.

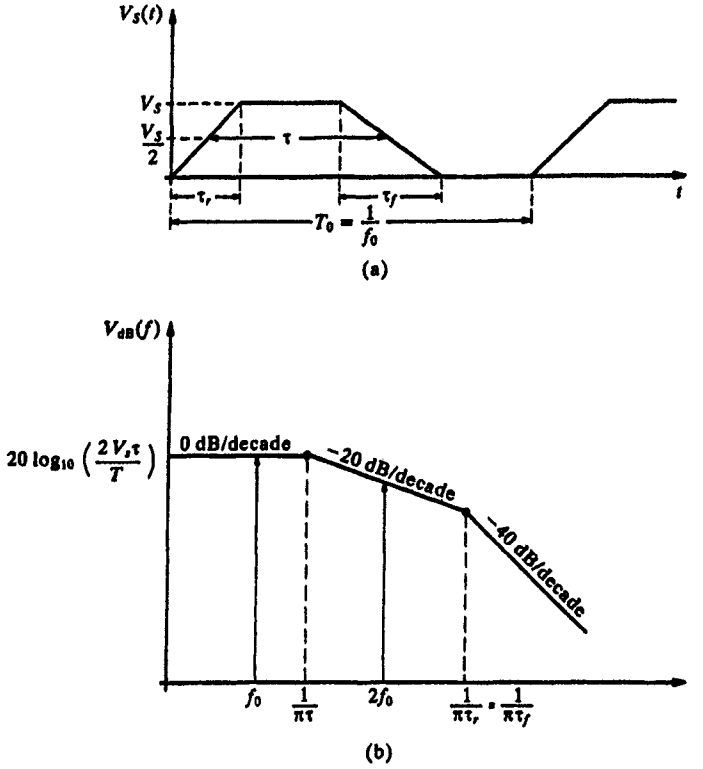

FIGURE 6.7 The frequency-domain representation of a periodic, trapezoidal pulse train.

$$\frac{d}{dt} V_S(t) \cong \frac{[V_S(t - T) - V_S(t - 3T)]}{2T} \tag{6.62b}$$

and the results in (6.60) are identical to those in (6.59).

The question of how much greater than the line one-way delay must be than the rise/fall times of the pulse in order to satisfy (6.61) can be answered in the following way. Consider $V_S(t)$ as being a periodic train of trapezoidal pulses with period T (repetition frequency $f = 1/T$) as illustrated in Fig. 6.7(a). The pulses have amplitude V_S, rise/fall times of τ_r, τ_f and pulse width τ between the 50% points. This is a common approximation to digital signals such as clock or data [A.3]. Suppose that the *risetime and falltime are identical*, i.e., $\tau_r = \tau_f$. In this case, the signal can be represented as a Fourier series as [A.3]

$$V_S(t) = V_S \frac{\tau}{T} + \sum_{n=1}^{\infty} c_n \cos\left(2\pi \frac{t}{T} + \phi_n\right) \tag{6.63}$$

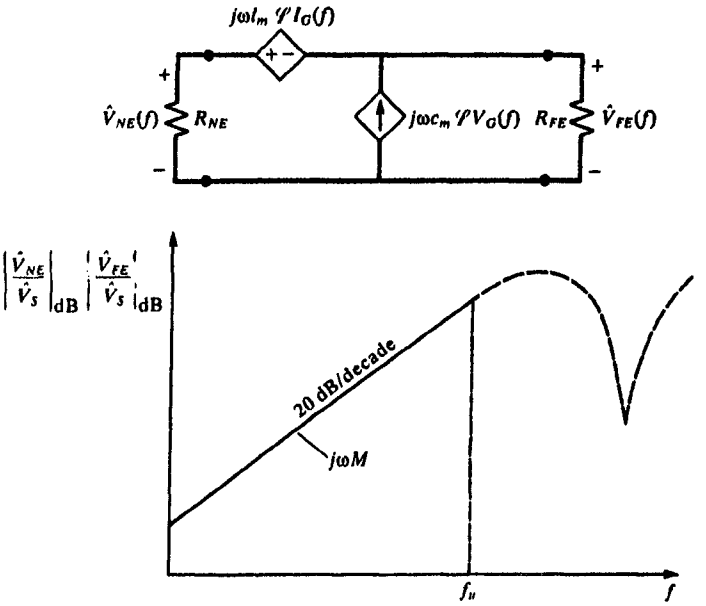

FIGURE 6.8 The frequency-domain transfer function predicted by the inductive-capacitive coupling model.

where

$$c_n = 2V_S \frac{\tau}{T} \frac{\sin(n\pi\tau/T)}{n\pi\tau/T} \frac{\sin(n\pi\tau_r/T)}{n\pi\tau_r/T} \tag{6.64a}$$

$$\phi_n = -n\pi\left(\frac{\tau + \tau_r}{T}\right) \tag{6.64b}$$

It is possible to obtain *bounds* on these magnitudes as shown in Fig. 6.7(b) [A.3]. These bounds consist of three line segments: one with slope 0 dB/decade out to a frequency of $1/\pi\tau$, one with slope -20 dB/decade from this point out to a frequency of $1/\pi\tau_r$, and one with slope -40 dB/decade thereafter. The high-frequency spectral content of the pulse is therefore primarily governed by the pulse rise/fall time. Consider the basic assumption of the low-frequency model as shown in Fig. 6.8: the frequency-domain crosstalk increases linearly with frequency (20 dB/decade) up to some frequency, f_u, where the line becomes electrically long. Combining the pulse spectrum in Fig. 6.7 and the crosstalk transfer function in Fig. 6.8 gives the resulting spectrum of the crosstalk pulse shown in Fig. 6.9. Observe in Fig. 6.9 that the high-frequency spectrum of the crosstalk pulse rolls off at -20 dB/decade. Let us choose the upper limit of validity for the low-frequency model, f_u, sufficiently greater than the beginning of this slope, $1/\pi\tau_r$, in order to assure that the higher frequency components

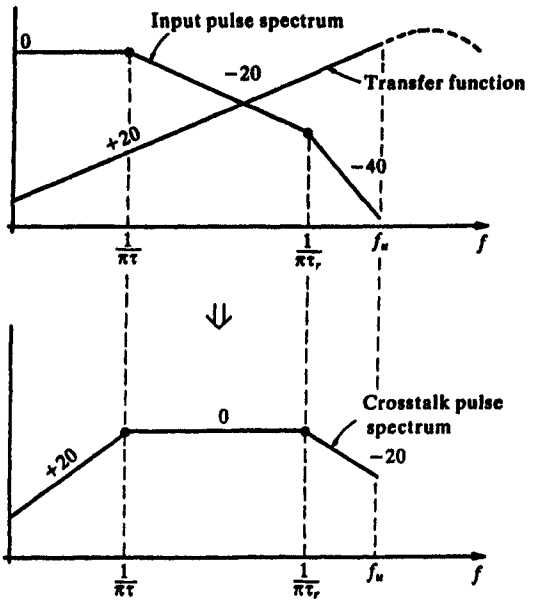

FIGURE 6.9 Combination of Figs. 6.7 and 6.8 to yield the frequency spectrum of the crosstalk voltages.

above f_u, which are not properly processed by the low-frequency model, will not be significant:

$$f_u \gg \frac{1}{\pi\tau_r} \tag{6.65}$$

Substituting f_u in terms of some fraction of line length, say, one-tenth:

$$\mathscr{L} = \frac{\lambda_u}{10} = \frac{1}{10}\frac{v}{f_u} \tag{6.66}$$

gives

$$\tau_r \gg \frac{10}{\pi}\frac{\mathscr{L}}{v} = 3.18T \tag{6.67}$$

Therefore the pulse rise/fall times must be larger than the line one-way delay. Typically choosing $\tau_r > 10T$ provides sufficient accuracy.

6.2.4 Common-Impedance Coupling

The effect of the impedance of the reference conductor can be handled in an approximate manner at the lower frequencies of the pulse by simply adding the

common-impedance coupling term to the inductive-capacitive contributions in (6.59):

$$V_{NE,FE}(t) = (M^{IND}_{NE,FE} + M^{CAP}_{NE,FE}) \frac{dV_S(t)}{dt} + M^{CI}_{NE,FE} V_S(t) \tag{6.68}$$

where the M's are as given previously. The effect of common-impedance coupling is to add a scaled replica of $V_S(t)$ to the crosstalk resulting from inductive and capacitive coupling.

6.3 COMPUTED RESULTS

In this section we will give some computed results comparing the predictions of the SPICE MTL (exact) model, the lumped-pi model, and the inductive-capacitive coupling model developed in this chapter for three-conductor lines that were examined in the previous two chapters. In all models the conductors are considered to be lossless. For both structures, the SPICE subcircuit models were computed with the **SPICEMTL.FOR, SPICELPI.FOR** and **SPICELC.FOR** computer programs described in Appendix A and combined into one SPICE program for ease of plotting the results. The nodes at the input to the generator lines are designated as S1, S2, and S3, whereas the nodes at the near end of the receptor circuit are designated as NE1 (SPICE), NE2 (lumped-pi), and NE3 (inductive-capacitive coupling model). The termination impedances are all 50 Ω resistive, i.e., $R_S = R_L = R_{NE} = R_{FE} = 50\,\Omega$.

Predictions of the exact time-domain solution of (6.42) are compared to those of the explicit solution of (6.47) using 7 terms in [B.15]. This reference also gives comparisons with the finite difference–time domain model and the time-domain to frequency-domain model. The exact frequency-domain result of (6.17) has been verified on numerous occasions and will therefore not be used here.

6.3.1 A Three-Wire Ribbon Cable

The first configuration is a three-wire ribbon cable considered previously. The wires are #28 gauge stranded (7 × 36) and are separated by 50 mils. One of the outer wires is the reference conductor and the line is of total length 2 m as shown in Figs 4.13 and 4.14. The per-unit-length parameters were computed in Chapter 3 with the **RIBBON.FOR** computer program described in Appendix A. Figure 6.10 compares the frequency-domain predictions for all three models over the frequency range of 1 kHz to 100 MHz. The line is one wavelength (ignoring the dielectric insulations) at 150 MHz so we may consider it to be electrically short for frequencies below, say, 15 MHz. The lumped-pi model gives good predictions below 10 MHz, whereas the inductive-capacitive coupling

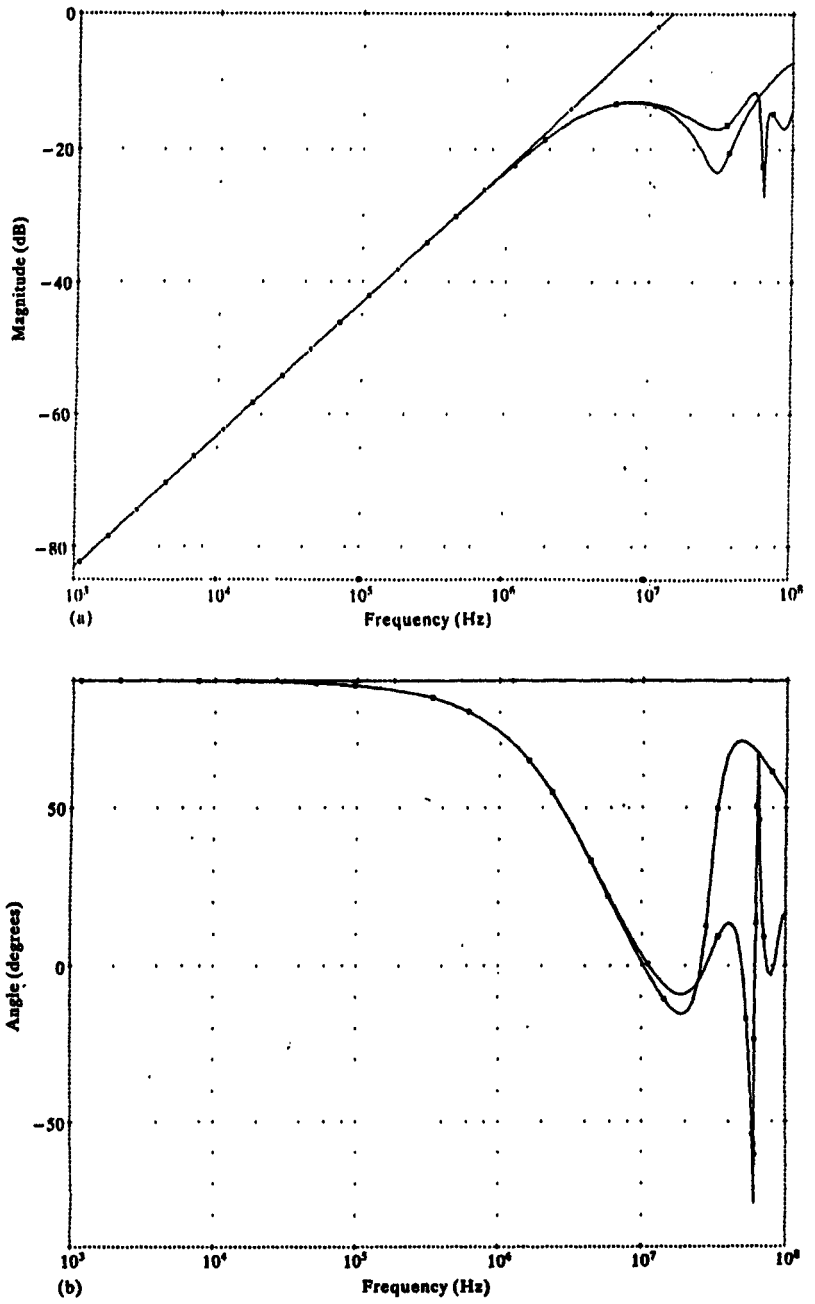

FIGURE 6.10 Illustration of the frequency response of the ribbon cable of Fig. 4.14 via the SPICE model, one lumped-pi section, and the inductive-capacitive coupling model. (a) Magnitude: □ VDB(NE1) – VDB(S1), ■ VDB(NE2) – VDB(S2), ◇ VDB(NE3) – VDB(S3). (b) Phase: □ VP(NE1) – VP(S1), ■ VP(NE2) – VP(S2), ◇ VP(NE3) – VP(S3).

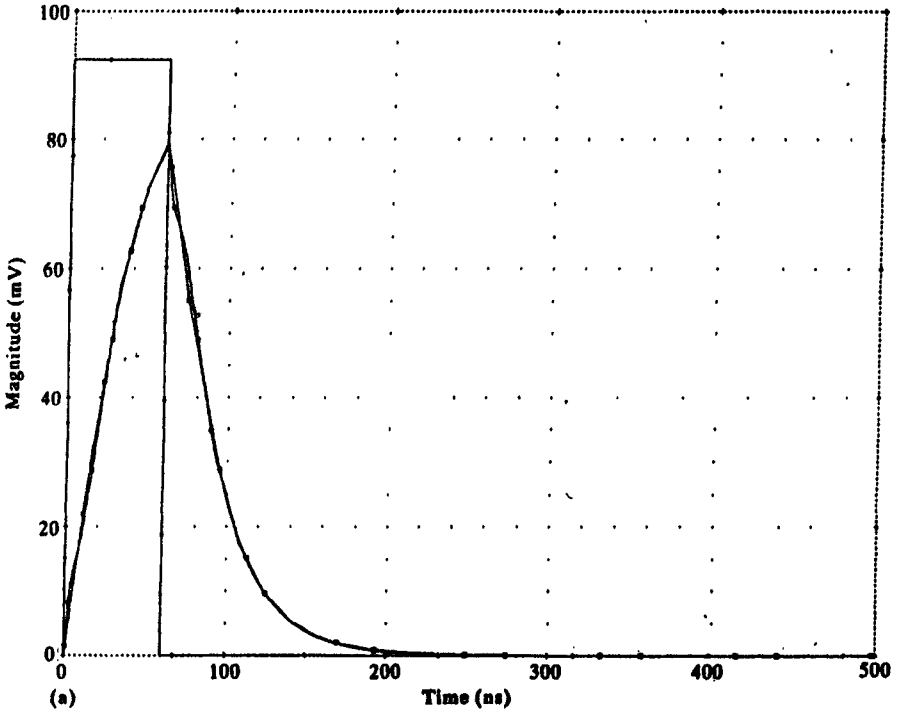

FIGURE 6.11 Illustration of the time-domain response of the ribbon cable of Fig. 4.14 via the SPICE model, one lumped-pi section, and the inductive-capacitive coupling model for a rise/fall time of (a), 60 ns.

model gives good predictions below 1 MHz. This shows that the simple inductive-capacitive coupling model can give adequate predictions for a significant frequency range so long as its basic limitations are observed.

Figure 6.11 shows the correlation between the three models for the time domain. The source, $V_S(t)$, is a 1 MHz trapezoidal pulse train with 50% duty cycle. The trapezoidal pulses have 1 V magnitude with various rise times. The one-way time delay for the line (ignoring the dielectric insulations) is $T = \mathscr{L}/v = 6.67$ ns so we should not expect the inductive-capacitive coupling model to give adequate predictions for risetimes less than, say, 60 ns. Figure 6.11(a) shows the predictions for $\tau_r = 60$ ns. The predictions of the lumped-pi model compare well with those of the SPICE model. Figure 6.11(b) shows the predictions for $\tau_r = 120$ ns, and Fig. 6.11(c) shows the predictions for $\tau_r = 240$ ns. Again, the predictions of the exact SPICE model and the lumped-pi model are excellent. For this latter risetime of 240 ns, there is good agreement between the inductive-capacitive coupling model's prediction of the peak crosstalk and $\tau_r = 36T$.

Figure 6.12 shows oscilloscope photographs of the experimental results. For

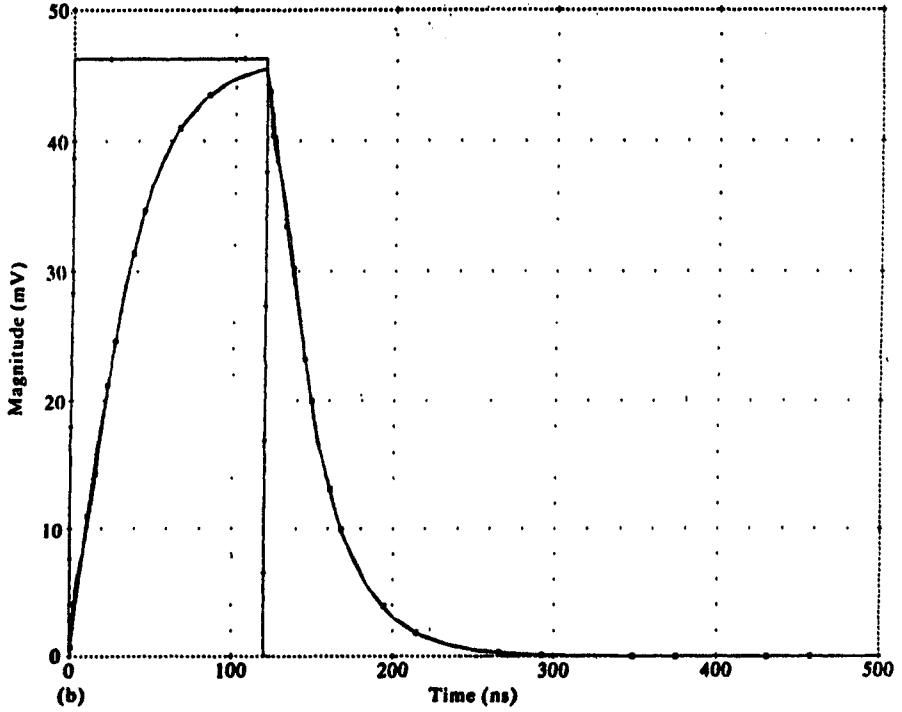

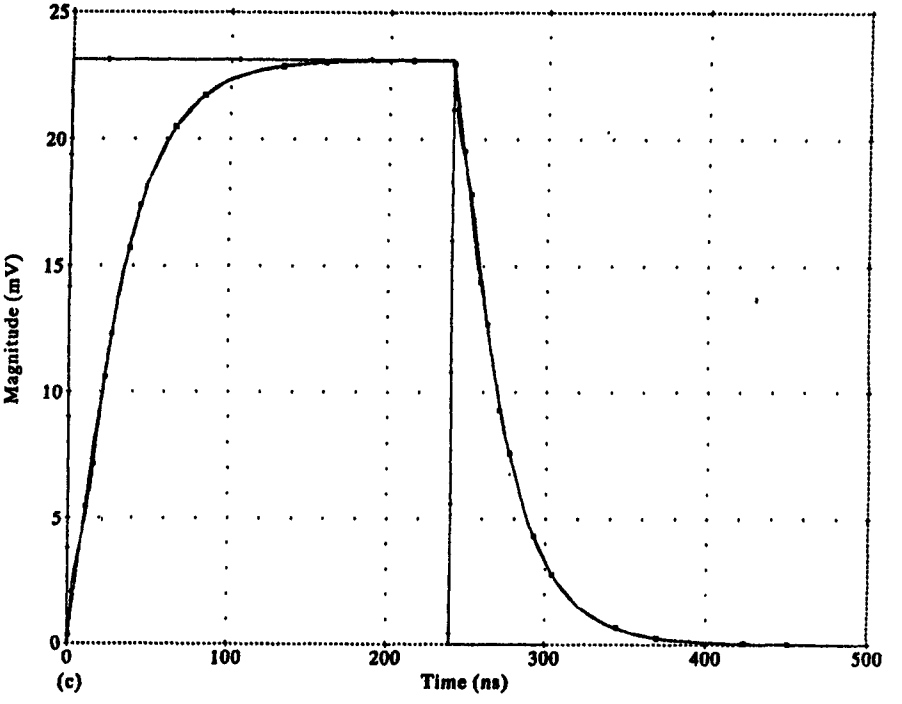

FIGURE 6.11 (*Continued*) (b) 120 ns, and (c) 240 ns. □ V(NE1), ■ V(NE2), ◇ V(NE3).

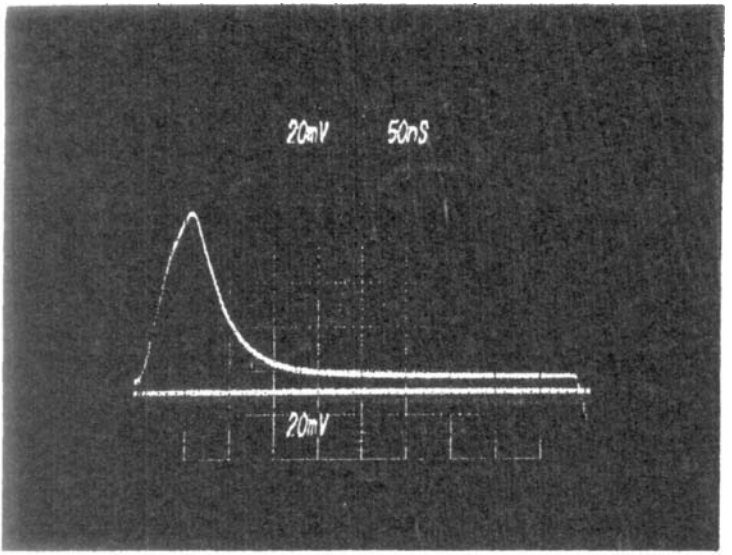

(a)

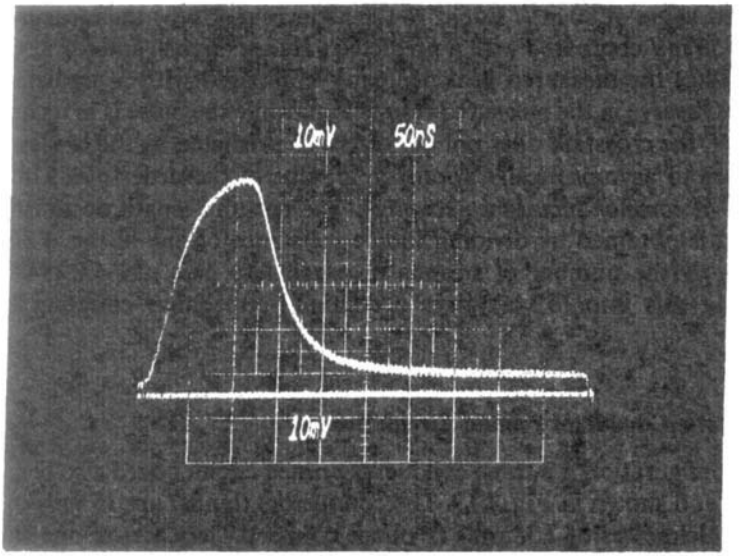

(b)

FIGURE 6.12 The experimentally determined time-domain response of the ribbon cable of Fig. 4.14 for a rise/fall time of (a) 60 ns, (b) 120 ns.

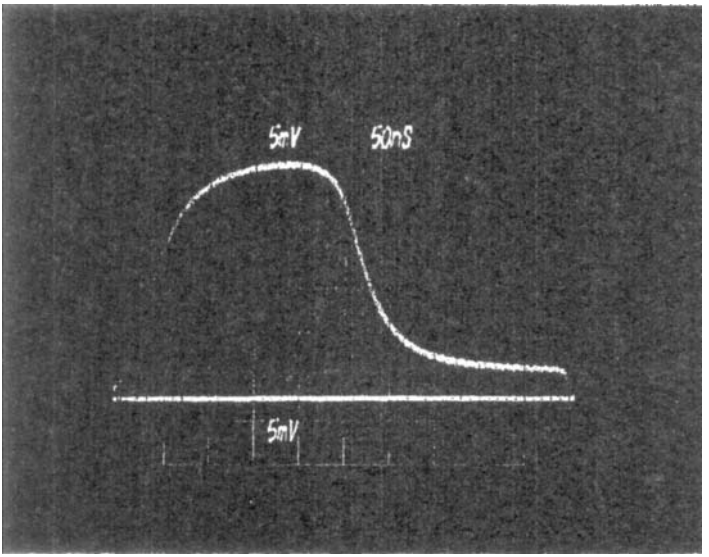

FIGURE 6.12 (*Continued*) (c) 240 ns.

$\tau_r = 60$ ns in Fig. 6.12(a) the measured peak voltage is 80 mV compared with a predicted value of 80 mV. For $\tau_r = 120$ ns in Fig. 6.12(b) the measured peak voltage is 50 mV compared with a predicted value of 45 mV, and for $\tau_r = 240$ ns in Fig. 6.12(c) the measured peak is 26 mV compared with a predicted value of 23 mV. Observe in the measured results that, while the pulse is in its quiescent state of 1 V, the crosstalk does not go to zero as predicted by the lossless model but appears to asymptotically approach a value of the order of 2.5 mV. This is a result of *common-impedance coupling*. The per-unit-length dc resistance of one strand is obtained by dividing the dc resistance of one of the #36 gauge strands by 7 (the number of strands in parallel to give $r\mathscr{L} = 0.194\,44\ \Omega/\text{m}$. Substituting this into (6.34a) gives a common-impedance coupling level of 1.94 mV.

6.3.2 A Three-Conductor Printed Circuit Board

The next configuration is a three-conductor printed circuit board also considered previously and shown in Fig. 4.17. The conductors (lands) are 15 mils in width and have thicknesses of 1.38 mils (1 ounce copper). They are on one side of a 47 mil thick glass epoxy board and have edge-to-edge separations of 45 mils. One of the outer lands is the reference conductor and the line is of total length 10 inches = 0.254 m. The per-unit-length parameters were computed in Chapter 3 with the **PCBGAL.FOR** computer program described in Appendix A. Figure 6.13 compares the frequency-domain predictions for all three models over the

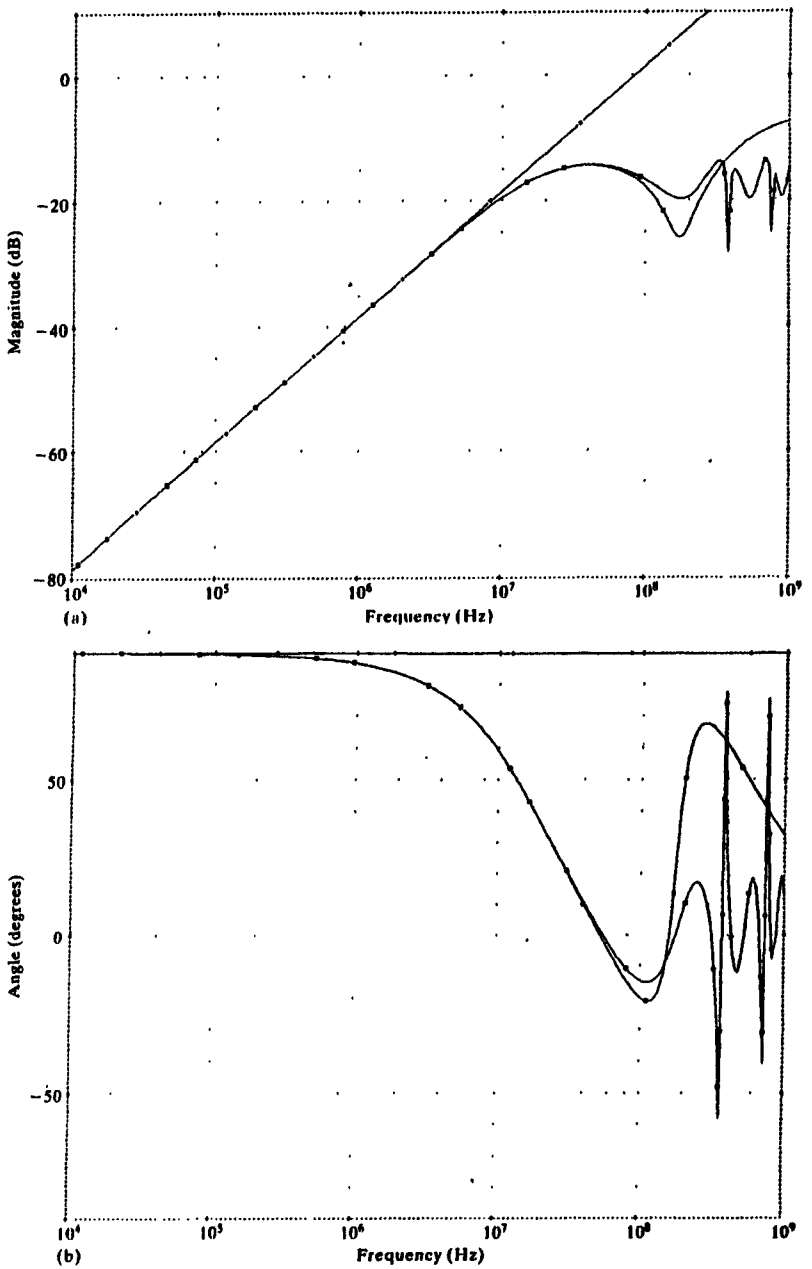

FIGURE 6.13 Illustration of the frequency response of the printed circuit board of Fig. 4.17 via the SPICE model, one lumped-pi section, and the inductive-capacitive coupling model. (a) Magnitude: ◇ VDB(NE1) – VDB(S1), ■ VDB(NE2) – VDB(S2), ◇ VDB(NE3) – VDB(S3), (b) Phase: □ VP(NE1) – VP(S1), ■ VP(NE2) – VP(S2), ◇ VP(NE3) – VP(S3).

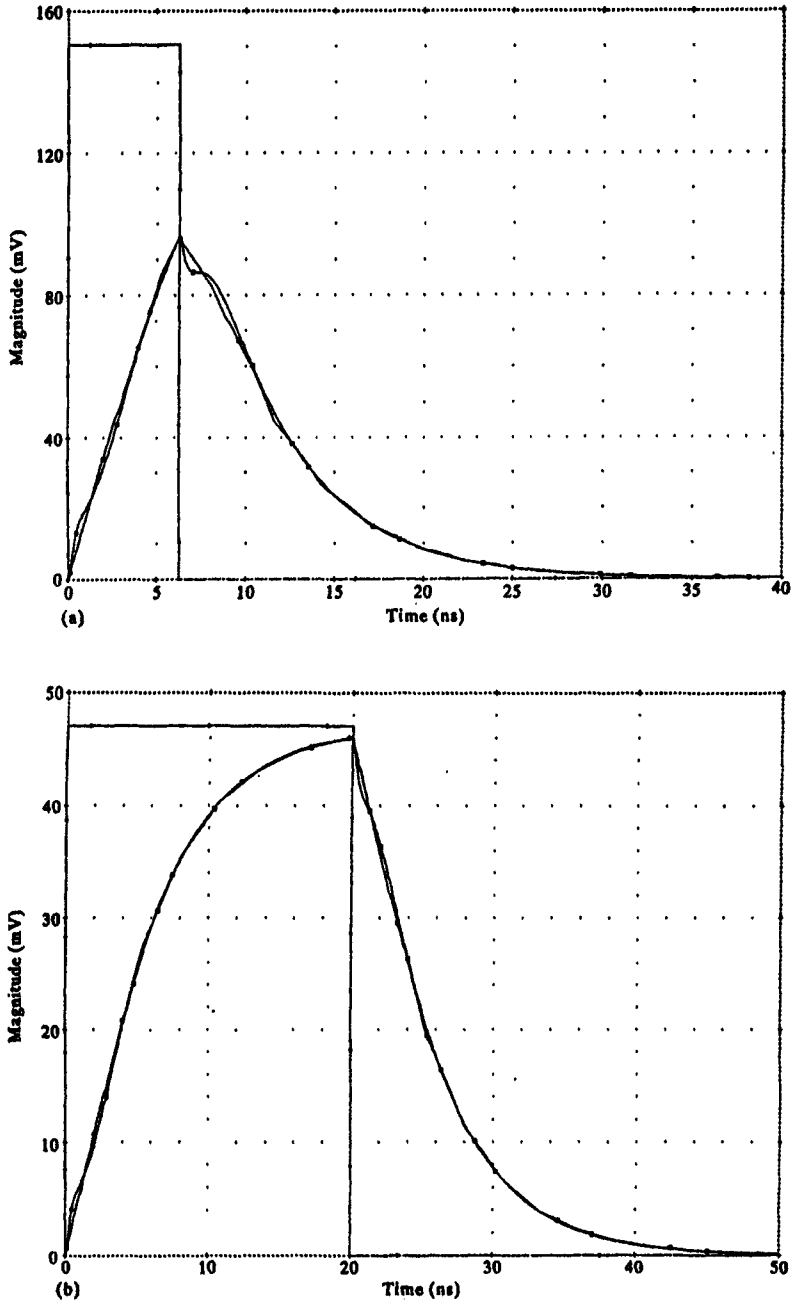

FIGURE 6.14 Illustration of the time-domain response of the printed circuit board of Fig. 4.17 via the SPICE model, one lumped-pi section, and the inductive-capacitive coupling model for a rise/fall time of (a) 6.25 ns, (b) 20 ns.

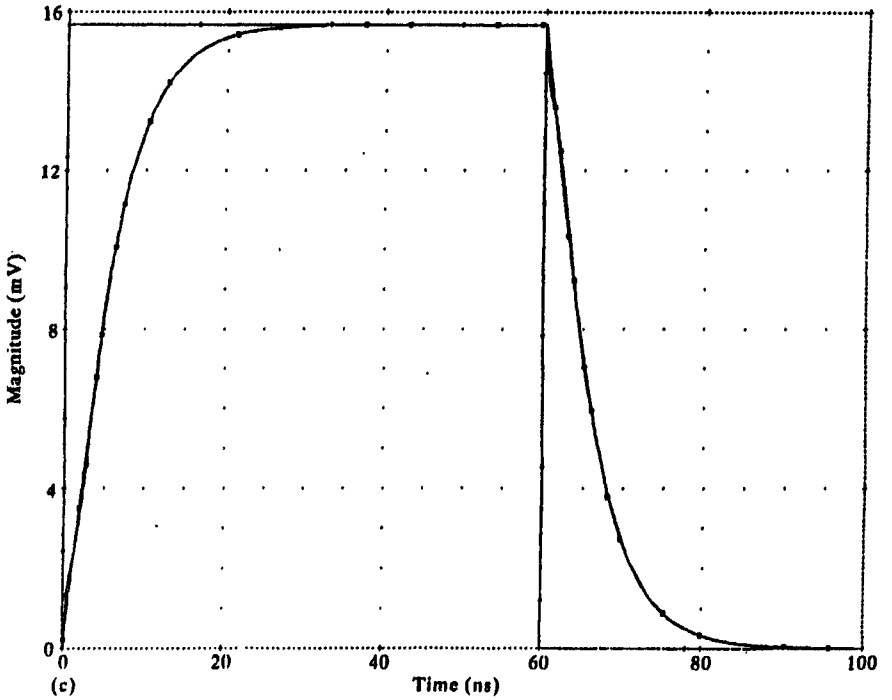

FIGURE 6.14 (*Continued*) (c) 60 ns.

frequency range of 10 kHz to 1 GHz. The line is one wavelength (ignoring the dielectric insulations) at 1.18 GHz so we may consider it to be electrically short for frequencies below, say, 100 MHz. The lumped-pi model gives good predictions below 100 MHz, whereas the inductive-capacitive coupling model gives good predictions below 10 MHz. This again shows that the simple inductive-capacitive coupling model can give adequate predictions for a significant frequency range so long as its basic limitations are observed.

Figure 6.14 shows the correlation between the three models for the time domain. The source, $V_S(t)$, is again a 1 V, 1 MHz trapezoidal pulse train with various risetimes. The one-way time delay for the line is (again ignoring the board dielectric) $T = \mathscr{L}/v = 0.85$ ns so we should not expect the inductive-capacitive coupling model to give adequate predictions for risetimes less than, say, 10 ns. Figure 6.14(a) shows the predictions for $\tau_r = 6.25$ ns. The predictions of the lumped-pi model compare well with those of the SPICE model. Figure 6.14(b) shows the predictions for $\tau_r = 20$ ns, and Fig. 6.14(c) shows the predictions for $\tau_r = 60$ ns. Again the predictions of the SPICE model and the lumped-pi model are virtually identical. For this latter risetime of 60 ns, the inductive-capacitive coupling model gives excellent prediction of the peak crosstalk magnitude and $\tau_r = 70T$.

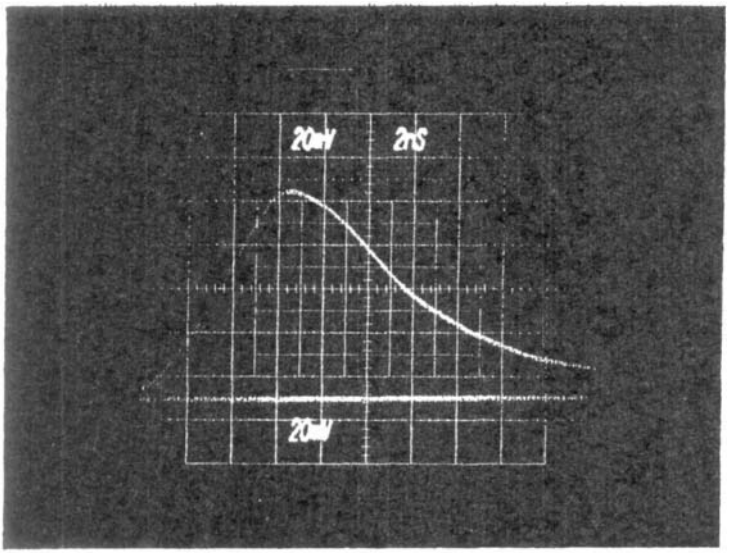

(a)

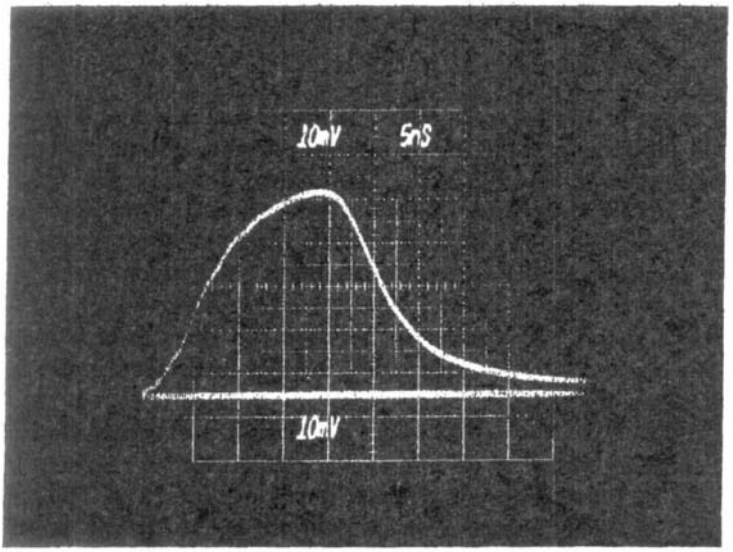

(b)

FIGURE 6.15 The experimentally determined time-domain response of the printed circuit board of Fig. 4.17 for a rise/fall time of (a) 6.25 ns, (b) 20 ns.

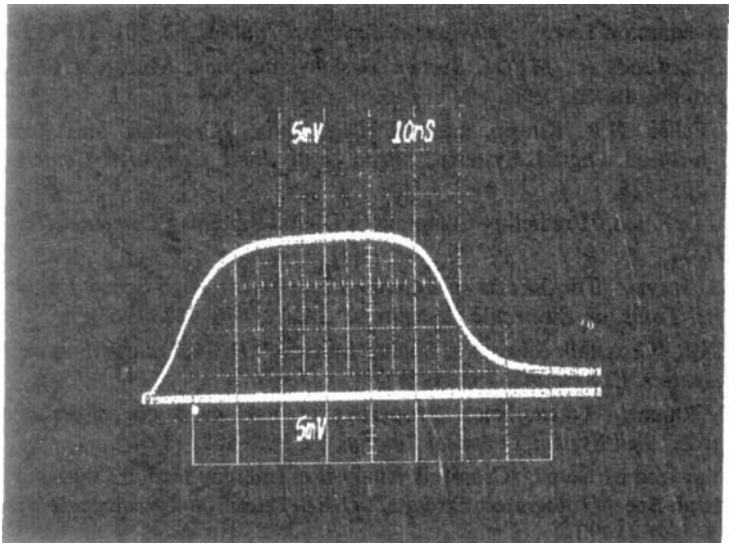

FIGURE 6.15 (*Continued*) (c) 60 ns.

Figure 6.15 shows oscilloscope photographs of the experimental results. For $\tau_r = 6.25$ ns in Fig. 6.15(a) the measured peak voltage is 94 mV compared with a predicted value of 95 mV. For $\tau_r = 20$ ns in Fig. 6.15(b) the measured peak voltage is 46 mV compared with a predicted value of 46 mV, and for $\tau_r = 60$ ns in Fig. 6.15(c) the measured peak is 17.5 mV compared with a predicted value of 15.8 mV. Observe in Fig. 6.15(c) that, again while the pulse is in its quiescent state of 1 V, the crosstalk does not go to zero as predicted by the lossless model but appears to asymptotically approach a value of the order of 2.5 mV. This shows that *common-impedance coupling* can be significant even for short conductors. The dc resistance of one land is $r\mathscr{L} = 0.3279\ \Omega/\text{m}$. Substituting this into (6.34a) gives a common-impedance coupling level of 1.64 mV.

REFERENCES

[1] L. Young, *Parallel Coupled Lines and Directional Couplers*, Artech House, Dedham, MA., 1972.

[2] V.K. Tripathi, "Asymmetric Coupled Transmission Lines in an Inhomogeneous Medium," *IEEE Trans. on Microwave Theory and Techniques*, **MTT-23**, 731–739 (1975).

[3] R. Speciale, "Even- and Odd-Mode Waves for Nonsymmetrical Coupled Lines in Nonhomogeneous Media," *IEEE Trans. on Microwave Theory and Techniques*, **MTT-23**, 897–908 (1975).

[4] J.C. Isaacs, Jr., and N.A. Strakhov, "Crosstalk in Uniformly Coupled Lossy Transmission Lines," *Bell System Technical Journal*, **52**, 101–115 (1973).

[5] W.R. Blood, Jr., *MECL System Design Handbook*, Motorola Semiconductor Products, 4th ed., 1988.

[6] A. Feller, H.R. Kaupp, and J.J. Digiacoma, "Crosstalk and Reflections in High-Speed Digital Systems," *Proc. Fall Joint Computer Conference*, 1965, pp. 511–525.

[7] J.A. DeFalco, "Predicting Crosstalk in Digital Systems," *Computer Design*, 69–75, (1973).

[8] D.B. Jarvis, "The Effects of Interconnections on High-Speed Logic Circuits," *IEEE Trans. on Electronic Computers*," **EC-12**, 476–487 (1963).

[9] I. Catt, "Crosstalk (Noise) in Digital Systems," *IEEE Transactions on Electronic Computers*, **EC-16**, 743–763 (1967).

[10] A.J. Rainal, "Transmission Properties of Various Styles of Printed Wiring Boards," *Bell System Technical Journal*, **58**, 995–1025 (1979).

[11] H. You and M. Soma, "Crosstalk Analysis of Interconnection Lines and Packages in High-Speed Integrated Circuits," *IEEE Trans. on Circuits and Systems*, **37**, 1019–1026 (1990).

PROBLEMS

6.1 Consider a problem consisting of two wires above an infinite, perfectly conducting plane. The wires are #28 gauge stranded wires (7 × 36) both at heights of 1 cm above the ground plane and separated by 100 mils (2.54 mm). Ignore the dielectric insulations. The terminations are $R_S = 50\,\Omega$, $R_L = 1\,\text{k}\Omega$, $R_{NE} = 300\,\Omega$, $R_{FE} = 100\,\Omega$. If the total line length is 2 m, compute the near-end and far-end frequency-domain crosstalk (magnitude and angle) using (6.17) from 1 kHz to 100 MHz. Determine the coupling coefficient, the near-end and far-end crosstalk coefficients, $M^{IND}_{NE,FE}$ and $M^{CAP}_{NE,FE}$, and the frequency where the line is 0.1λ long.

6.2 For the structure of Problem 6.1, repeat the crosstalk calculations using the low-frequency, inductive-capacitive coupling model in (6.29).

6.3 For the structure of Problem 6.1, assume that $V_S(t)$ is a 1 MHz, periodic train of trapezoidal pulses with equal rise/fall times of 100 ns and a level of 1 V. Compute the time-domain near-end and far-end crosstalk using the iterative solution given in (6.42). Repeat these calculations for rise/fall times of 50 ns and 10 ns.

6.4 Repeat Problem 6.3 using the explicit solution given in (6.47).

6.5 Repeat Problem 6.3 using the low-frequency, inductive-capacitive coupling approximation given in (6.59).